Applied Water Science (2020) 10:40
https://doi.org/10.1007/s13201-019-1124-4

ORIGINAL ARTICLE

Decolorization of Rhodamine B dye by using multiwalled carbon nanotubes/Co–Ti oxides nanocomposite and Co–Ti oxides as photocatalysts

Noor Zada[1] · Khalid Saeed[1,2] · Idrees Khan[1,2]

Received: 14 November 2019 / Accepted: 16 December 2019 / Published online: 26 December 2019

Abstract
Functionalized multiwalled carbon nanotubes (F-MWCNTs)/Co–Ti oxide nanocomposites and neat Co–Ti oxide nanoparticles were synthesized by chemical reduction method. The scanning electron microscopy micrographs show that the bimetallic NPs in F-MWCNTs/Co–Ti are present in dispersed form while the neat Co–Ti nanoparticles were found in agglomerated form. The formation of nanocomposites and neat Co–Ti nanoparticles was also confirmed by energy-dispersive X-ray. Both types of nanocomposites were employed as photocatalyst for the photodegradation of Rhodamine B in aqueous medium under UV light irradiation. The photodegradation study was performed via UV–Vis spectrophotometer. The photodegradation results show that F-MWCNTs/Co–Ti oxide NPs degraded about 93.35% dye within 150 min irradiation time while the neat Co–Ti oxide NPs degraded about 91.76% dye within same irradiation time. The F-MWCNTs/Co–Ti can be easily removed and recycled due to its bulky composite nature as compared to neat Co–Ti oxide NPs. The effect of dye concentration, catalyst dosage, pH of medium and activity of recycled catalyst was also evaluated.

Keywords Multiwalled carbon nanotubes · Bimetallic nanoparticles · Photodegradation · Rhodamine B · Cobolt · Titanium

Introduction

Bimetallic nanoparticles are a type of nanoparticles (NPs) which consist of two different metals that show a combination of properties that are associated with the two constituent metals (Devi and Singh 2016). Bimetallic NPs exhibit unique properties as compared to their pure individual NPs. They have a wide range of magnetic, biomedical and catalytic applications. They have a tunable optical behavior and also play a vital role in bio-sensing (Devi et al. 2016). Among various types of bimetallic NPs, bimetallic alloy NPs have higher catalytic efficiency than their monometallic counterparts due to strong synergy between the metals (Devi and Singh 2016). Different bimetallic NPs were reported as photocatalyst for the photodegradation of organic pollutants such as NiO–Ag bimetallic NPs for methyl violet (Devi et al. 2016). Metal and their oxide NPs were utilized as good heterogeneous photocatalysts due to its chemical stability, low corrosion and high surface area (Saeed and Khan 2017). Among the metal oxides, TiO_2 is the most suitable photocatalyst (Riaz et al. 2012) due to its relatively high photocatalytic efficiency, nontoxicity, long-term stability, photosensitivity, low toxicity, antimicrobial properties and low cost and thus widely employed in wastewater treatment (Souza and Corio 2013; Koo et al. 2014). It is chemically and biologically inert, non-corrosive, photocatalytically stable and has high oxidative ability (Kerkez and Boz 2015). TiO_2 represents low photocatalytic activity due to its wide band gap, high electron–hole pair recombination rate and also its excitation only under UV light wavelength (Benjume et al. 2012). Various approaches have been practiced to retard its charge recombining deficiency such as depositing noble metals like Pt or Pd on TiO_2 surface (Saeed et al. 2017), doping other metal such as magnesium on TiO_2 surface (Avasarala et al. 2016) and combining TiO_2 with other metal oxides such as ZrO_2 to form nanoconjugates (Benjume et al. 2012). Nanoconjugates also called mixed oxide composites have more efficient photocatalytic activity

✉ Idrees Khan
idreeschem_uom@yahoo.com

[1] Department of Chemistry, University of Malakand, Chakdara, Dir (L), Khyber Pakhtunkhwa, Pakistan

[2] Department of Chemistry, Bacha Khan University, Charsadda, Khyber Pakhtunkhwa, Pakistan

than pure substances through the generation of new active sites, thermal stability, improved mechanical strength and surface area of titania. The active surface area and adsorption capacity in this system are greatly increased to the dye molecules (Smirnova et al. 2015). Various metal oxides such as ZnO, Al_2O_3, MnO_2, ZrO_2, Ta_2O_5 and In_2O_3 have been coupled with TiO_2 and were found to be efficiently increased its photocatalytic activity (Benjume et al. 2012).

In the present study, cobalt-coupled titania nanoconjugate is synthesized through chemical reduction method with and without F-MWCNTs. The F-MWCNTs not only increase the surface area of bimetallic NPs (generally present in agglomerated form), but also have the ability to store and shuttle electrons in order to separate h^+/e^- pairs (Li et al. 2013), which ultimately increase its photocatalytic activity. F-MWCNTs are reported as support materials for the synthesis of bimetallic nanoparticles (Saeed et al. 2018). These F-MWCNTs/Co–Ti and Co–Ti NPs were used as photocatalyst for the photodegradation of Rhodamine B dye under UV light irradiation in aqueous medium as a function of irradiation time, catalyst dosage, dye concentrations and pH of the media. The effect of recovered catalyst was also studied. The Rhodamine B dye is selected due to its solubility in water and mainly used as colorant in food stuffs, textiles and a well-known fluorescent water tracer. It is very harmful if swallowed by human beings and animals and causes irritation to eyes, skin and respiratory tract (Sangami and Dharmaraj 2012). Various studies were carried out on the degradation of Rhodamine B dye, but mostly of these studies show long irradiation time and hard reaction conditions and operations (Kumar and Kumar 2019; Lops et al. 2019; Xiao et al. 2019). In our studies, RB dye was degraded in 150 min with a very simple reaction condition and operation.

Experimental work

Chemicals and materials

$CoCl_2.6H_2O$ and $TiCl_4$ were purchased from the Merck and BDH companies, respectively, and used as received. Analytical-grade nitric acid, sulfuric acid and sodium hydroxide were purchased from Scharlau Company. The MWCNTs were supplied by Nanomirea and manufactured by thermal chemical vapor deposition. The diameter and length of the CVD MWNTs were 20–40 nm and 30–40 µm, respectively, and its purity was higher than 95%. Rhodamine B dye was supplied by Sigma-Aldrich.

Acid treatment of MWCNTs

The MWCNTs, 100 mL HNO_3 (6 M) and 100 mL H_2SO_4 (2 M) were taken in reaction flask and sonicated for 30 min. The mixture was refluxed at 170 °C for 6 h and then cooled with constant stirring. The acid-treated MWCNTs are then cooled to room temperature, separated by filtration and then washed several times with distilled water in order to remove the unreacted acids. The F-MWCNTs are dried in oven at 110 °C and stored for further use.

Synthesis of F-MWCNTs/Co–Ti oxides and Co–Ti oxide NPs

100 mL of 0.1 M concentration from both $CoCl_2.6H_2O$ and $TiCl_4$ solutions and 0.5 g of F-MWCNTs were taken in conical flask and stirred on magnetic stirrer. The mixture is then basified by dropwise adding NaOH (1 M) until pH reached 10 with constant stirring. The mixture is then sonicated (full volume at 30 °C) for 30 min through sonicator for complete dispersion of F-MWCNTs in the solution. The obtained mixture was then refluxed at 70 °C for 2 h with occasionally stirring for better dispersion of nanotubes and deposition of NPs on F-MWCNT surface. The final mixture was cooled, centrifuged (10,000 rpm for 30 min), washed with distilled water and dried in oven at 100 °C to get the F-MWCNTs/Co–Ti oxide NPs. The ratio between components in the F-MWCNTs/Co–Ti oxide NPs is (F-MWCNTs:Co:Ti) 0.5:0.9:0.7. The same procedure was used for the preparation of Co–Ti oxide NPs except adding F-MWCNTs.

Photodegradation of Rhodamine B dye

The photocatalytic activity of the prepared F-MWCNTs/Co–Ti oxides and Co–Ti oxide NPs was evaluated by using it as photocatalysts against Rhodamine B (RB) dye. In the time study, 0.02 g of F-MWCNTs/Co–Ti oxide NPs and 0.01 g of Co–Ti oxide NPs are added separately to 10 mL of RB dye (20 ppm) in 50-mL beakers and sealed with colorless cover to permit penetration of light radiation and to stop water evaporation. The samples were placed in dark for 30 min in order to attain adsorption–desorption equilibrium. The solution mixture was then kept under UV light with constant stirring for a given irradiation time. After specific time of UV irradiation, the photocatalyst was separated out from the RB dye aqueous solution by using centrifugation (10,000 rpm for 10 min) through centrifuge machine (models 1–14). The effect of recovered catalyst, catalyst dosage, dye concentrations and pH of the media on the photodegradation of RB was also evaluated. The general scheme of photodegradation study is shown in Fig. 1. The photodegradation study of the RB dye was monitored by using UV–visible spectrophotometer, and the percent degradation of was calculated by the following formula (Saeed and Khan 2017):

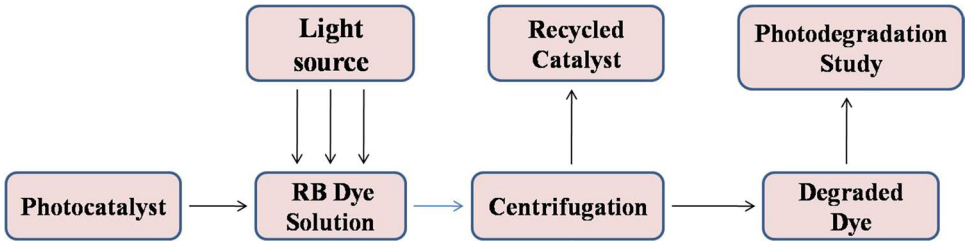

Fig. 1 General scheme of photodegradation of RB dye

$$\text{Degradation Rate } (\%) = \frac{C_o - C}{C_o} \times 100$$

$$\text{Degradation Rate } (\%) = \frac{A_o - A}{A_o} \times 100$$

where C_o is the initial dye concentration, C is the dye concentration after UV irradiation, A_o shows initial absorbance and A shows the dye absorbance after UV irradiation.

Instrumentations

The morphological study was performed by scanning electron microscopy (SEM) model no. JEOL-Jsm-5910; JEOL Company, Japan. The energy-dispersive X-ray (EDX) study was performed by EDX spectrometer model Inea 200, UK. Centrifugation was performed using centrifuge machine (Wise Spin Model: CF-10). The photodegradation study was monitored by UV/VIS spectrophotometer (Shimadzu 160 A, Japan).

Results and discussion

Morphological and elemental composition study

The surface morphological study is very important for analyzing the surface area as it is directly related with the catalytic activity while compositional study provides information about the particular material synthesis and its purity. Figure 2a, b shows the SEM images of F-MWCNTs/Co–Ti oxides and Co–Ti oxide NPs, respectively. The micrographs presented that NPs (Fig. 2b) are mostly present in spherical shape in the form of agglomeration. The micrograph (Fig. 2a) also illustrated that NPs are present in dispersed form on the F-MWCNTs surface. The synthesis of F-MWCNTs/Co–Ti oxides and Co–Ti oxide NPs is also confirmed by their EDX spectra. Figure 3a, b shows the EDX spectra's of F-MWCNTs/Co–Ti oxides and Co–Ti oxide NPs, respectively. The figure shows that Co and Ti are present in large quantity in both the photocatalysts. The presence of carbon peak in Fig. 3a is for the F-MWCNTs while the presence of oxygen peak in Fig. 3a, b confirms that bimetallic NPs are formed in their oxide form. The presence of oxygen peak in Fig. 2a also confirms the functionalization of MWCNTs by acid treatment, which introduces carboxyl functional group.

Photodegradation study of Rhodamine B

The prepared F-MWCNTs/Co–Ti oxides and Co–Ti oxide NPs were used as photocatalysts for the photocatalytic degradation of Rhodamine B (RB) dye under UV light irradiation. Figure 4a, b shows the UV–visible spectra of RB in an aqueous medium in the presence of F-MWCNTs/Co–Ti oxides and Co–Ti oxide NPs, respectively, as a function of irradiation time. The photodegradation of RB was measured from the relative intensity of its UV–Vis spectra, which gave a maximum absorbance peak at 554 nm. Photodegradation is achieved when UV light falls upon the bimetallic NPs that results in the excitation of electrons (e^-) from the valence band of NPs to its conduction band, and creates a positive

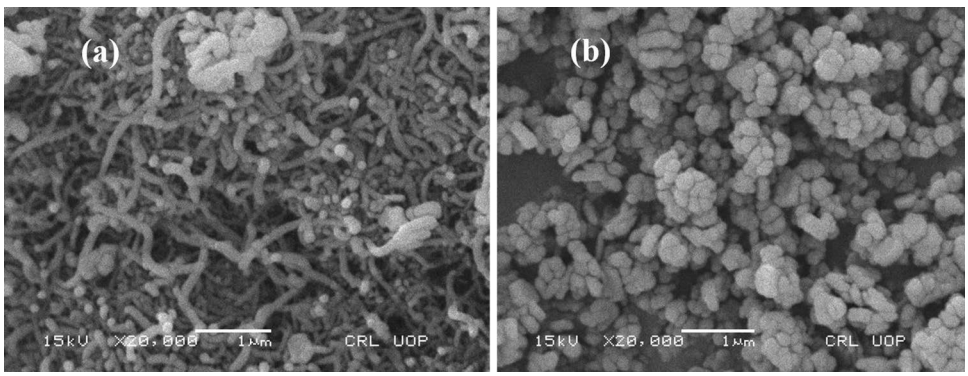

Fig. 2 SEM images of **a** F-MWCNTs/Co–Ti oxides and **b** Co–Ti oxide NPs

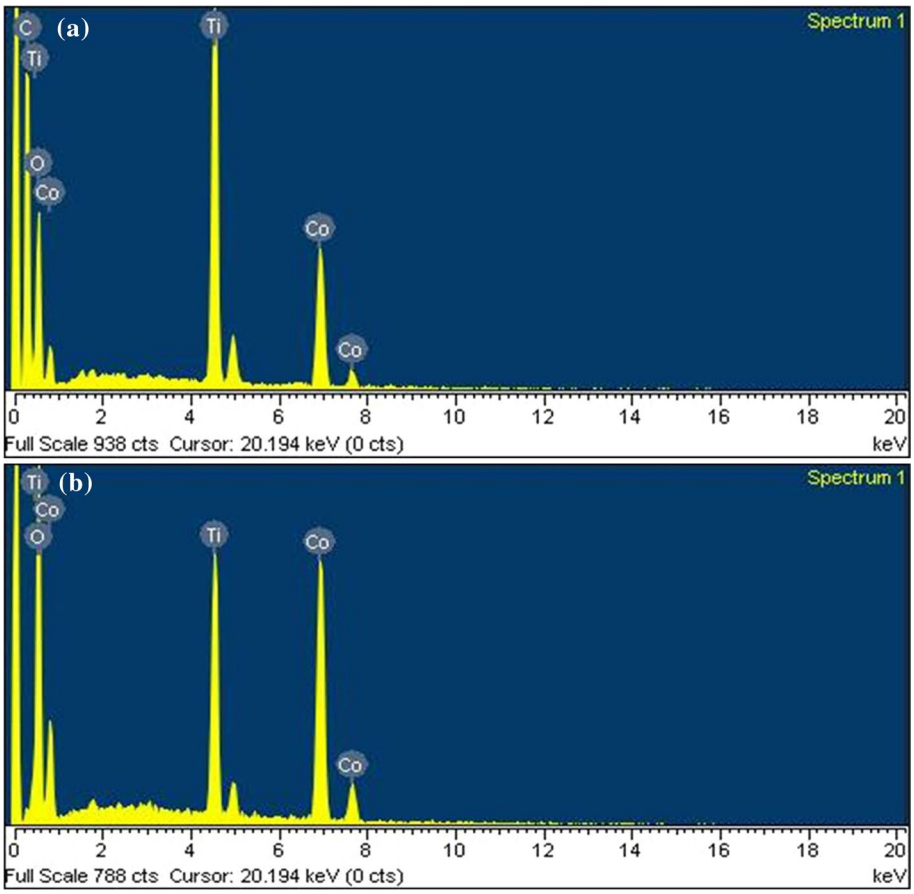

Fig. 3 EDX spectra of **a** F-MWCNTs/Co–Ti oxides and **b** Co–Ti oxide NPs

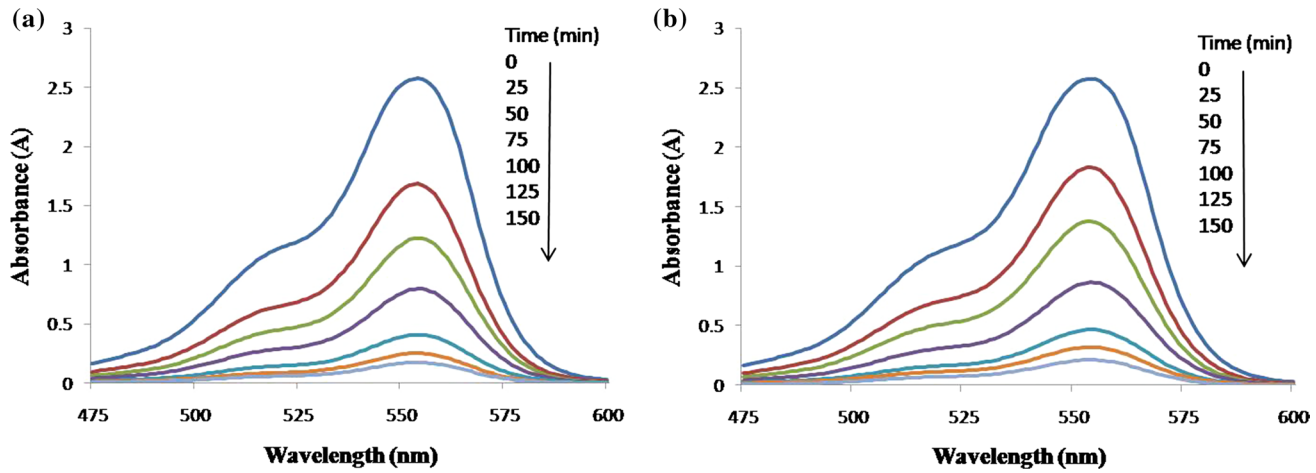

Fig. 4 UV–Vis spectra of RB dye before and after UV light irradiation photodegraded by **a** F-MWCNTs/Co–Ti oxide NPs and **b** Co–Ti oxide NPs

hole (h^+) in the valence band. The conduction band e^- is captured and stored by the F-MWCNTs, hence reducing the recombining deficiencies of the created charges, while in the unsupported bimetallic NPs greater quantity of these separated charges recombines. This e^- trapping and storing property of F-MWCNTs makes it suitable for NP support which increases NP catalytic activity as compared to unsupported NPs. The electron in the conduction band or stored in MWCNTs is trapped by the O_2 molecule to form a reactive superoxide anion radical ($\dot{O}_2^-$), while the h^+ present in the

valence band reacts with water molecule and forms hydroxyl radicals ($^{\cdot}OH$). These radicals created are highly reactive toward photodegradation of dye [Saeed and Khan 2017; Li et al. 2013). The proposed mechanism is easily understood from Fig. 5. The following steps summarize the mechanism:

$$CNTs/NPs \rightarrow CNTs\ (e^{-}) + NPs\ (h^{+})$$

$$CNTs\ (e^{-}) + O_2 \rightarrow CNTs + {}^{\cdot}O_2^{-}$$

$$NPs\ (h^{+}) + OH^{-} \rightarrow NPs + {}^{\cdot}OH$$

$$Dye + {}^{\cdot}OH \rightarrow \text{degradable products}$$

$$Dye + {}^{\cdot}O_2^{-} \rightarrow \text{degradable products}$$

Figure 6a shows the comparison of the %degradation of RB dye in the presence of F-MWCNTs/Co–Ti oxides and Co–Ti oxide NPs, respectively. The results show that with increasing irradiation time the photodegradation of dye also increases. From the result, it is clear that at initial irradiation time of 25 min the F-MWCNTs/Co–Ti oxides degraded about 34.61% dye which increases to 52.4, 69.11, 84.18, 90.24 and 93.35% as irradiation time increased to 50, 75, 100, 125 and 150 min, respectively. Similarly, the Co–Ti oxide NPs degraded about 28.86, 46.54, 66.43, 81.89, 87.64 and 91.76% within irradiation time of 25, 50, 75, 100, 125 and 150 min. The results show that F-MWCNTs/Co–Ti oxides degraded the dye more rapidly than Co–Ti oxide NPs. Figure 6b shows a plot of lnCo/C versus irradiation time, representing a linear relationship, which indicates pseudo-first-order kinetics. The values of correlation coefficient (R^2) are also represented in Fig. 6b.

The used catalyst is washed many times with excess of distilled water in order to remove the adsorbed dye and used as photocatalysts under the same experimental conditions for evaluating its recycled efficiency. Figure 7a, b shows the UV–visible spectra of RB in an aqueous medium in the presence of recycled F-MWCNTs/Co–Ti oxides and Co–Ti oxide NPs, respectively, as a function of irradiation time. The results revealed that the recovered F-MWCNTs/Co–Ti oxides degraded more dye than the recovered Co–Ti oxide

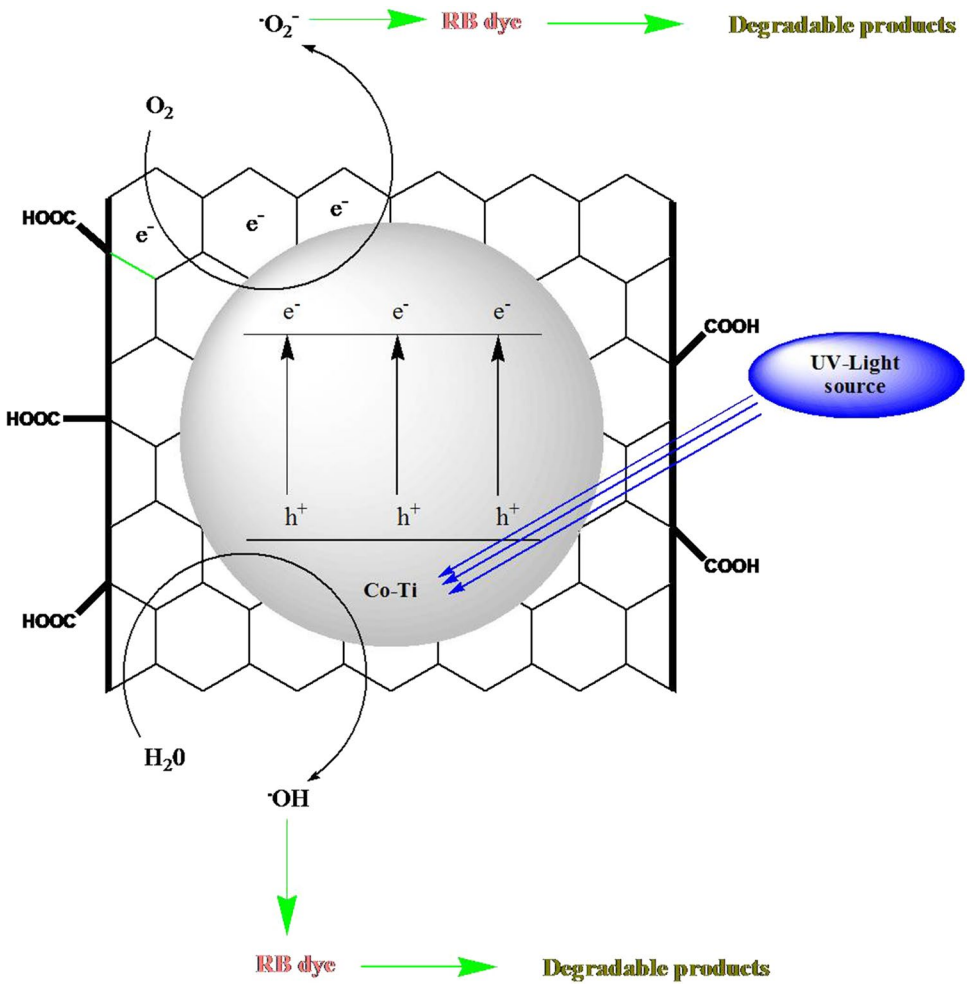

Fig. 5 General proposed mechanism for CR dye photodegradation

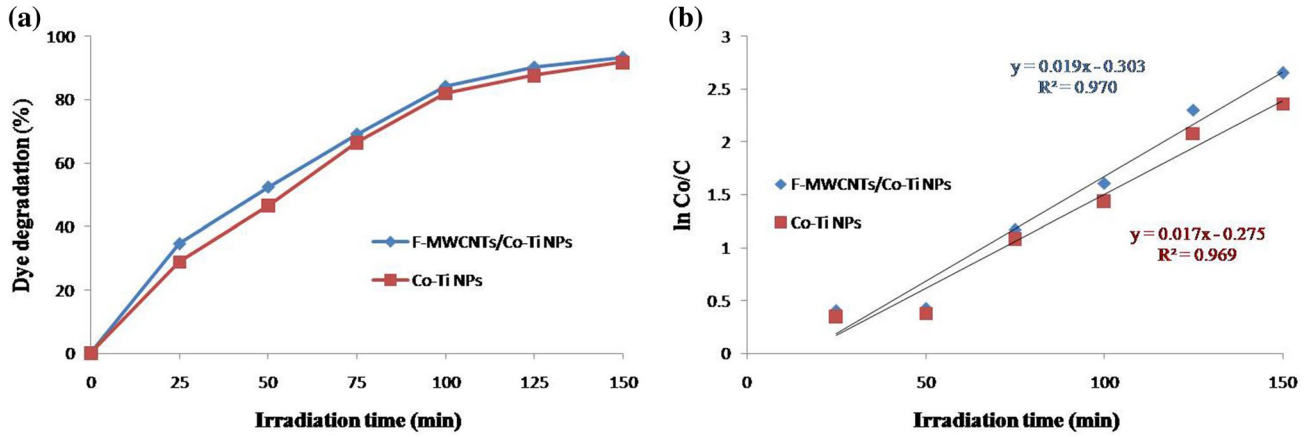

Fig. 6 **a** Comparison of %degradation of RB dye by F-MWCNTs/Co–Ti oxides and Co–Ti oxide NPs and **b** kinetics study

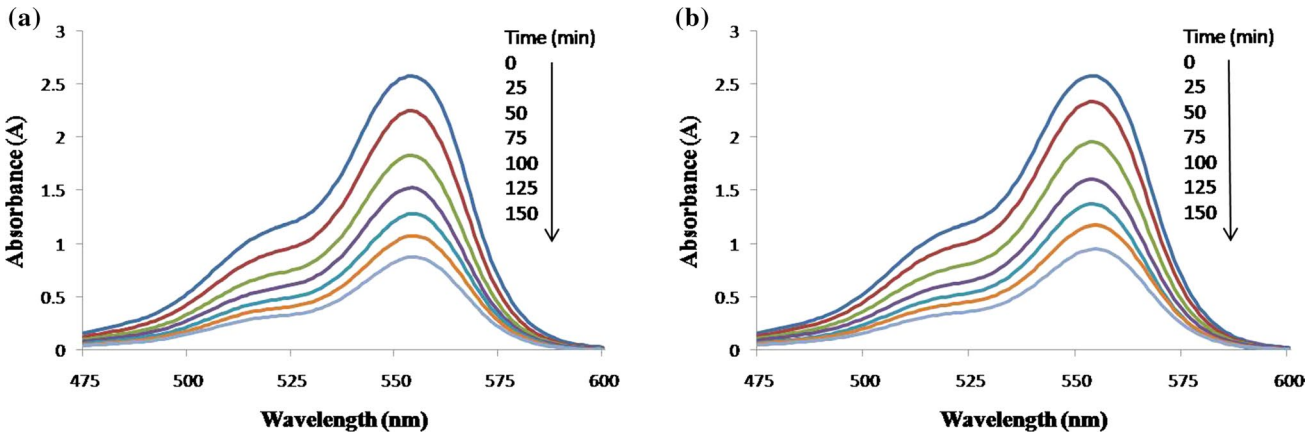

Fig. 7 UV–Vis spectra of RB dye under UV light irradiation in the presence of recovered **a** A-MWCNTs/Co–Ti oxide NPs and **b** Co–Ti oxide NPs

NPs like the original photocatalysts. Figure 8a shows the comparison of the %degradation of RB dye photodegraded by original and recovered F-MWCNTs/Co–Ti oxide NPs. The results show that the original F-MWCNTs/Co–Ti oxides degraded less dye than recovered F-MWCNTs/Co–Ti oxides within each irradiation time. Within 25 min irradiation time, the fresh F-MWCNTs/Co–Ti oxides degraded 34.61% while the recovered degraded 12.7%. Within the maximum irradiation time of 150 min, the fresh F-MWCNTs/Co–Ti oxides degraded about 93.35% dye while the recovered degraded about 66% dye. Figure 8b shows the comparison of %degradation of RB dye photodegraded by original and recovered Co–Ti oxide NPs. The results data confirmed that the original Co–Ti oxide NPs degraded 28.86% dye within 25 min irradiation time while the recovered Co–Ti oxide NPs degraded about 9.32% dye; by increasing irradiation time to 150 min the original photocatalyst degraded about 91.76% dye while the recovered degraded about 62.97% dye.

Effect of the photocatalyst amount

Catalyst amount plays a vital role in dye degradation because different amounts of catalyst provide a different number of active sites. The effect of photocatalyst dosage on photocatalysis of RB was also monitored by loading different dosages/amounts of F-MWCNTs/Ag–Co oxide NPs (0.08, 0.13, 0.18, 0.23 and 0.28 g) and Ag–Co oxide NPs (0.02, 0.07, 0.12, 0.17 and 0.22 g) under constant irradiation time of 100 min and 20 ppm dye concentration. Figure 9a, b shows the UV–visible spectra of RB dye before and after UV light irradiation in an aqueous medium photodegraded by different amounts of F-MWCNTs/Co–Ti oxides and Co–Ti oxide NPs, respectively. The result shows that as photocatalyst amount increases, photodegradation of dye also increases. Figure 10 shows the comparison of the %degradation of RB dye photodegraded by F-MWCNTs/Co–Ti oxides and Co–Ti oxide

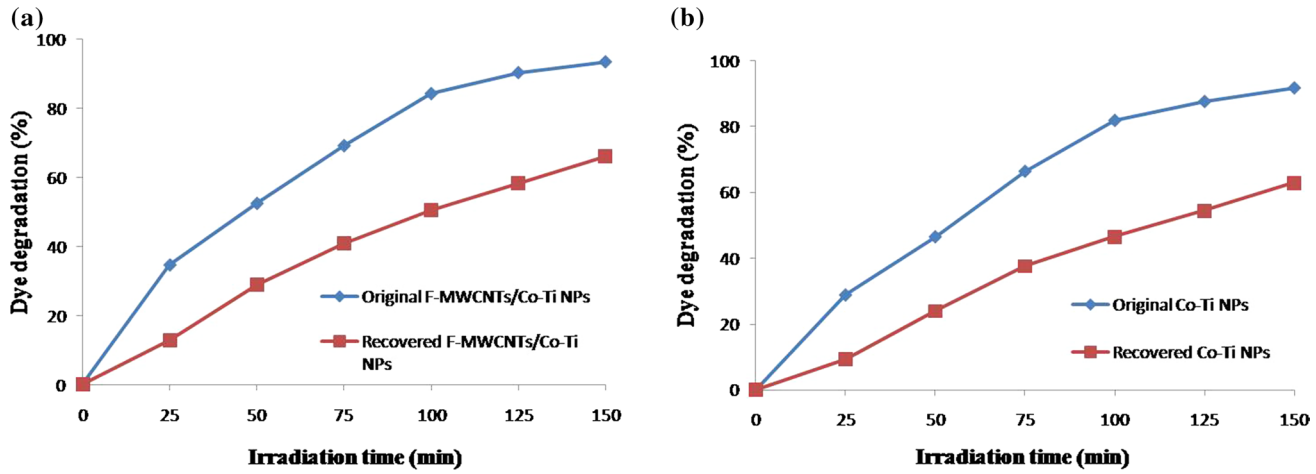

Fig. 8 Comparison of the %degradation of RB dye by original and recovered **a** A-MWCNTs/Co–Ti oxide NPs and **b** Co–Ti oxide NPs

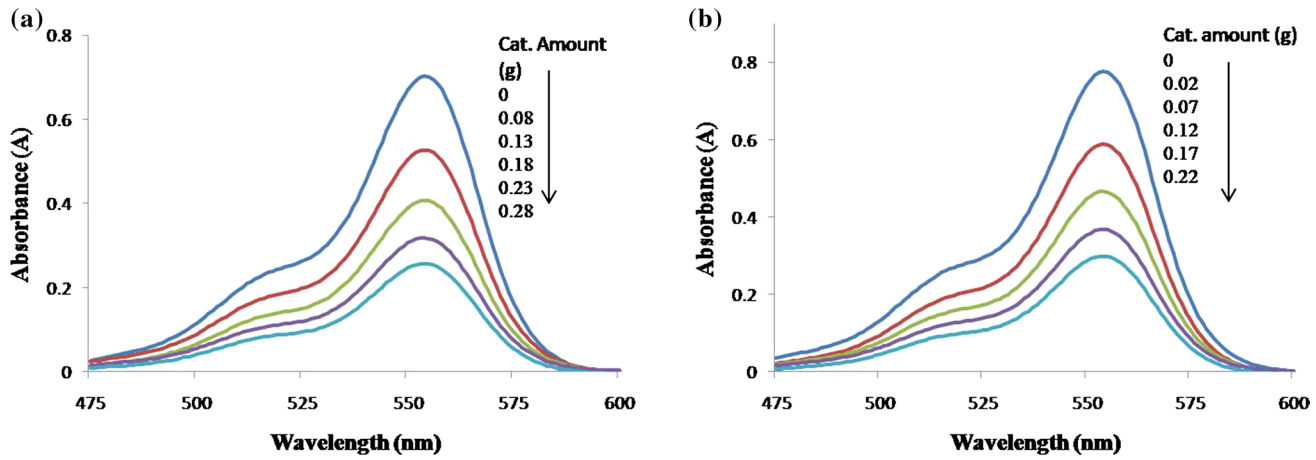

Fig. 9 UV–Vis spectra of RB dye under UV light irradiation at different amounts of **a** A-MWCNTs/Co–Ti oxides and **b** Co–Ti oxide NPs

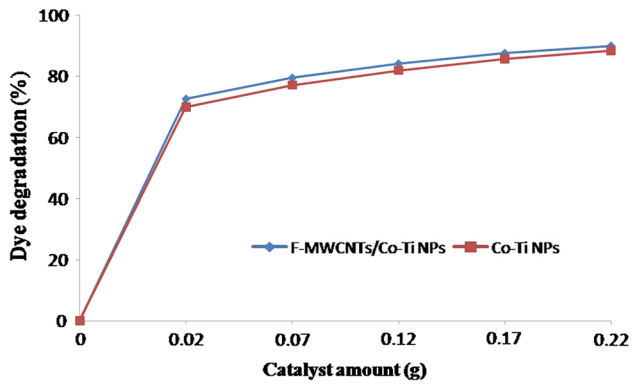

Fig. 10 %Degradation comparison of RB dye by different amounts of A-MWCNTs/Co–Ti oxides and Co–Ti oxide NPs

NPs. Figure 10 confirms that the F-MWCNTs/Co–Ti oxides degraded more dye than Co–Ti oxide NPs. The results confirmed that 0.08 g of F-MWCNTs/Ag–Co oxide NPs degrades about 72.64% dye, which increases to 90.01% by increasing to the maximum dosage of 0.28 g. Similarly, 0.02 g of Ag–Co oxide NPs degraded 69.85% dye while increasing catalyst dosage to 0.22 g photodegradation of RB dye increases to 88.38%. The results show that increasing catalyst up to certain limit rate of degradation increases and then increasing catalyst amount beyond that limit levels off the photodegradation rate. The reason for this phenomenon is that increasing catalyst amount increases quantity of photons adsorbed which consequently enhances the photodegradation rates. On the other, further increase in catalyst dosage beyond the limit increases solution opacity leading to decrease in photon penetration, hence decreasing photodecomposition rate (Reza et al. 2017).

Effect of initial dye concentration

As industries discharge dyes at various concentrations, the effect of initial RB dye concentration on the photodegradation rate was evaluated by studying the RB photodegradation in different dye concentrations (10, 15, 20, 25 and 30 ppm) keeping irradiation time (100 min) and catalyst amount (0.02 g of F-MWCNTs/Co–Ti oxide NPs and 0.01 g of Co–Ti oxide NPs) constant. The effect of the initial RB dye concentration on the photodegradation rate is shown in Fig. 11, which shows the comparison of %degradation of RB dye by constant amount of F-MWCNTs/Co–Ti oxides and Co–Ti oxide NPs. The results show that the maximum dye degradation was occurred in the lower initial dye concentration. Results data revealed that in the presence of F-MWCNTs/Co–Ti oxide NPs at 10 ppm, a maximum degradation of 92.79% was achieved while increasing concentration to 15, 20, 25 and 30 ppm, photodegradation decreases in ascending order of 87.26, 84.18, 81.5 and 80.7%, respectively. This decrease in dye degradation occurs at higher initial dye concentration because more and more dye molecules will be adsorbed on photocatalyst surface and significant amount of UV light will be absorbed by the dye molecules rather than the photocatalyst; consequently, light penetration to NP surface decreases. Due to this phenomenon, generation of hydroxyl radicals decreases as the active sites were occupied by dyes, and hence, photodegradation rate decreases (Reza et al. 2017). Similarly, Co–Ti oxide NPs degraded about 90.99% dye at 10 ppm which also decreases to 84.83, 81.89, 80.71 and 79.91% by increasing initial dye concentration to 15, 20, 25 and 30 ppm, respectively.

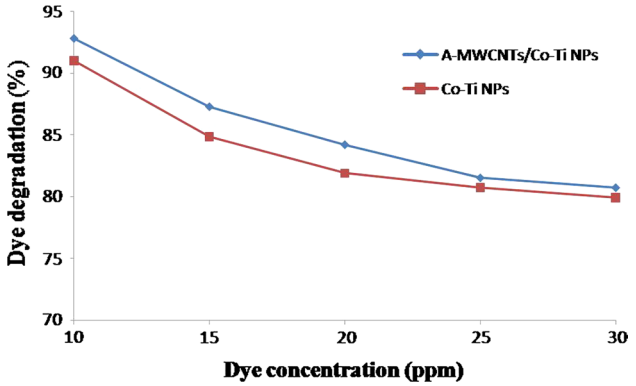

Fig. 11 Comparison of %degradation of RB dye at different initial dye concentrations at constant amount of A-MWCNTs/Co–Ti oxides and Co–Ti oxide NPs

Effect of pH of the medium

Various industries discharge their effluents at different pHs, and therefore, it is necessary to study the effect of pH on the degradation of organic dyes. Figure 12a, b shows the UV–visible spectra of RB dye before and after UV light irradiation photodegraded by F-MWCNTs/Co–Ti oxides and Co–Ti oxide NPs, respectively. The effect of pH was studied by preparing the dye solution in different pH media and studying under constant initial dye concentration (20 ppm) irradiation time (100 min) and catalyst dosage (0.02 g of F-MWCNTs/Co–Ti oxide NPs and 0.01 g of Co–Ti oxide NPs). Figure 13 shows the comparison of the %degradation of RB dye photodegraded by F-MWCNTs/Co–Ti oxides and Co–Ti oxide NPs in different pH media. The result shows that pH has a low effect on the photodegradation rate on RB dye; however, greater degradation is achieved at higher pH. This higher photodegradation rate in the basic medium may be attributed to the enhanced

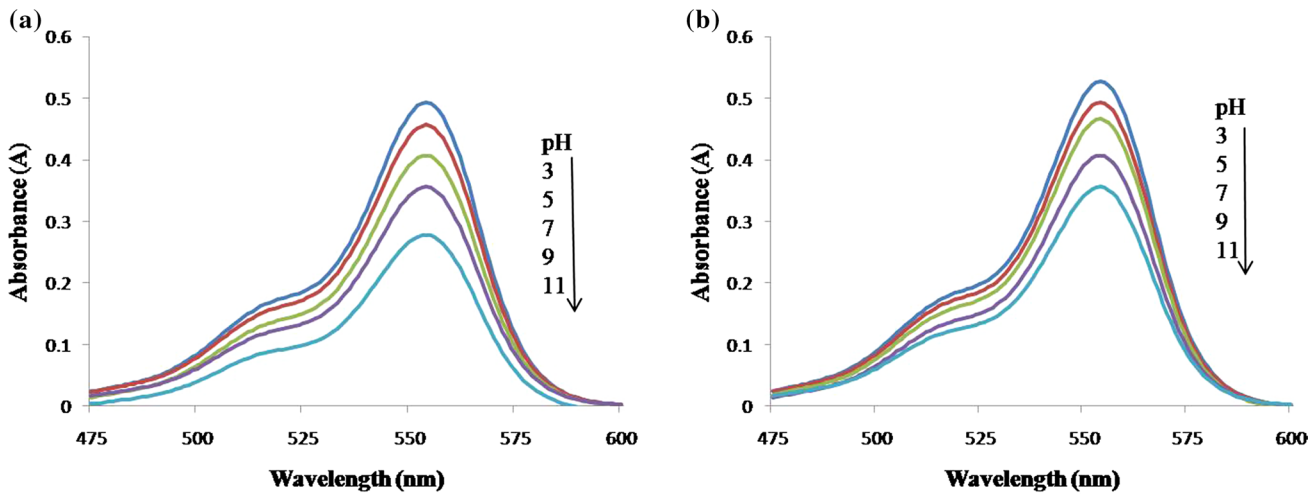

Fig. 12 UV–Vis spectra of RB dye under UV light irradiation in the presence of A-MWCNTs/Co–Ti oxides and Co–Ti oxide NPs in different pH media

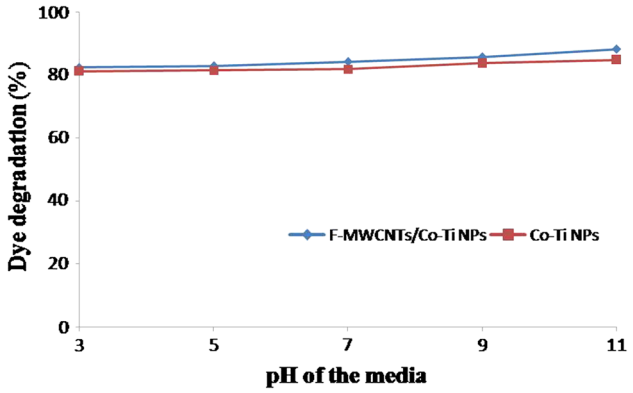

Fig. 13 Comparison of %degradation of RB dye photodegraded by A-MWCNTs/Co–Ti oxides and Co–Ti oxide NPs in different pH media

formation of hydroxyl radicals which is a strong oxidizing species (Saeed et al. 2016). The results show that at pH 3 the F-MWCNTs/Co–Ti oxides degraded 82.38%, which increases up to 88.16% by increasing pH to 11. Similarly, the Co–Ti oxide NPs degraded about 81.16% dye at pH 3, which increases to 81.5, 81.89, 83.7 and 84.83% by increasing pH of the media to 5, 7, 9 and 11, respectively.

Conclusion

F-MWCNTs increase the photocatalytic activity of bimetallic NPs because of its ability to trap and store the conduction band electron and hence reduce the recombining deficiencies of the separated charges. Acid treatment of MWCNTs improves its dispersive properties as well as strengthens its interaction with metal NPs. The F-MWCNT-supported Co–Ti oxides were found more effective in the degradation of RB dye as compared to unsupported NPs in aqueous media due to high surface area of the well-dispersed NPs on F-MWCNTs and the synergistic effect between bimetallic NPs and F-MWCNTs. The increase in the rate of photodegradation with increasing photocatalysts dosage up to certain limit is due to the availability of more active sites. The photodegradation rate was found higher in basic medium due to the generation of more hydroxyl radicals in the basic medium. The faster photodegradation rate at low initial dye concentration is due to small quantity of dye molecules and easy penetration of UV light. The recycled photocatalysts also significantly degraded AR dye but show less activity as compared to fresh catalyst due to the blocking of its active sites.

Funding The University of Malakand, Chakdara, Dir (L), Khyber Pakhtunkhwa, Pakistan, and Bach Khan University, Charsadda, Khyber Pakhtunkhwa, Pakistan, supported our research work (Grant No. 1).

Compliance with ethical standards

Conflict of interest The authors declare that they have no conflict of interest.

References

Avasarala BK, Tirukkovalluri SR, Bojja S (2016) Magnesium doped titania for photocatalytic degradation of dyes in visible light. J Environ Anal Toxicol 6:1000358

Benjume MLG, Cabrera MIE, Garcıa MEC (2012) Enhanced photocatalytic activity of hierarchical macro-mesoporous anatase by ZrO_2 incorporation. Int J Photoenergy. https://doi.org/10.1155/2012/609561

Devi HS, Singh TD (2016) Cu–Zn and Cu–Ni bimetallic particles fabricated using ascorbic acid and its role in photodegradation of methyl orange. Asian J Chem 28:2255–2260

Devi HS, Singh TD, Singh HP (2016) Tailoring of bimetallic NiO–Ag nanoparticles for degradation of methyl violet through a benign approach. J Mat Res 31:3459–3471

Kerkez O, Boz I (2015) Photodegradation of methylene blue with Ag_2O/TiO_2 under visible light: operational parameters. Chem Eng Commun 202:534–541

Koo Y, Littlejohn G, Collins B, Yun Y, Shanov VN, Schulz M, Pai D, Sankar J (2014) Synthesis and characterization of Ag–TiO_2–CNT nanoparticle composites with high photocatalytic activity under artificial light. Compos Part B Eng 57:105–111

Kumar PTKM, Kumar ASK (2019) Visible-light-induced degradation of rhodamine B by nanosized Ag2S–ZnS loaded on cellulose. Photochem Photobiol Sci 18:148–154

Li Z, Liu J, Zhang FJ, Oh WC (2013) UV and visible light photodegradation effect on Fe–CNT/TiO_2 composite catalysts. B Mater Sci 36:293–299

Lops C, Ancona A, Cesare KD, Dumontel B, Garino N, Canavese G, Hernandez S, Cauda V (2019) Sonophotocatalytic degradation mechanisms of Rhodamine B dye via radicals generation by micro- and nano-particles of ZnO. Appl Catal B Environ 243:629–640

Reza KM, Kurny ASW, Gulshan F (2017) Parameters affecting the photocatalytic degradation of dyes using TiO_2: a review. Appl Water Sci 7:1569–1578

Riaz N, Chong FK, Dutta BK, Man ZB, Khan MS, Nurlaela E (2012) Photodegradation of Orange II under visible light using Cu–Ni/TiO_2: effect of calcination temperature. Chem Eng J 185–186:108–119

Saeed K, Khan I (2017) Efficient photodegradation of neutral red chloride dye in aqueous medium using graphene/cobalt-manganese oxides nanocomposite. Turk J Chem 41:391–398

Saeed K, Khan I, Sadiq M (2016) Synthesis of graphene-supported bimetallic nanoparticles for the sunlight photodegradation of Basic Green 5 dye in aqueous medium. Sep Sci Technol 51:1421–1426

Saeed K, Khan I, Gul T, Sadiq M (2017) Efficient photodegradation of methyl violet dye using TiO_2/Pt and TiO_2/Pd photocatalysts. Appl Water Sci 7:3841–3848

Saeed K, Zada N, Khan I, Sadiq M (2018) Synthesis, characterization and photodegradation application of Fe–Mn and F-MWCNTs supported Fe–Mn oxides nanoparticles. Desalination Water Treat 108:362–368

Sangami G, Dharmaraj N (2012) UV–visible spectroscopic estimation of photodegradation of rhodamine-B dye using tin(IV) oxide nanoparticles. Spectrochim Acta A Mol Biomol Spectrosc 97:847–852

Smirnova NP, Surovtseva NI, Fesenko TV, Demianenko EM, Grebenyuk AG, Eremenko AM (2015) Photodegradation of dye acridine yellow on the surface of mesoporous TiO_2, SiO_2/TiO_2 and SiO_2 films: spectroscopic and theoretical studies. J Nanostructure Chem 5:333–346

Souza MLD, Corio P (2013) Effect of silver nanoparticles on TiO_2-mediated photodegradation of Alizarin Red S. Appl Catal B Environ 136–137:325–333

Xiao X, Ma XL, Liu ZY, Li WW, Yuan H, Ma XB, Li LX, Yu HQ (2019) Degradation of rhodamine B in a novel bio-photoelectric reductive system composed of Shewanella oneidensis MR-1 and Ag_3PO_4. Environ Int 126:560–567